

# Collapse of a Molecular Cloud Core to Stellar Densities: The First Three-Dimensional Calculations

Matthew R. Bate

*Max-Planck-Institut für Astronomie, Königstuhl 17, D-69117 Heidelberg, Germany*

## ABSTRACT

We present results from the first three-dimensional calculations ever to follow the collapse of a molecular cloud core ( $\sim 10^{-18} \text{ g cm}^{-3}$ ) to stellar densities ( $> 0.01 \text{ g cm}^{-3}$ ). The calculations resolve structures over 7 orders of magnitude in spatial extent ( $\sim 5000 \text{ AU} - 0.1 \text{ R}_\odot$ ), and over 17 orders of magnitude in density contrast. With these calculations, we consider whether fragmentation to form a close binary stellar system can occur during the second collapse phase. We find that, if the quasistatic core that forms before the second collapse phase is dynamically unstable to the growth of non-axisymmetric perturbations, the angular momentum extracted from the central regions of the core, via gravitational torques, is sufficient to prevent fragmentation and the formation of a close binary during the subsequent second collapse.

*Subject headings:* accretion – hydrodynamics – ISM: clouds – methods: numerical – stars: formation

## 1. Introduction

The formation of close binary stellar systems is an, as yet, unsolved problem in the field of star formation. Calculations following the isothermal collapse and fragmentation of molecular cloud cores can successfully produce binaries with separations  $\gtrsim 1$  AU (e.g. Boss 1986). However, once a collapsing molecular cloud core becomes optically thick, the gas temperature increases with density, a hydrostatic core is formed with radius  $\sim 4$  AU (Larson 1969), and fragmentation is suppressed (Boss 1986, 1988).

A potential opportunity to form close binaries via fragmentation occurs when the temperature in the hydrostatic core reaches  $\sim 2000$  K and molecular hydrogen begins to dissociate, resulting in a second collapse within the hydrostatic core (Larson 1969). When the dissociation is complete, the collapse is finally stopped with the formation of a second hydrostatic, or stellar, core. Fragmentation during the second collapse has been obtained by Boss (1989) and Bonnell & Bate (1994), although in the former paper the binary quickly merged. In both papers, fragmentation was found to occur only if the ratio of the rotational energy to the magnitude of the gravitational potential energy,  $\beta$ , exceeded the value required for dynamic instability to non-axisymmetric perturbations ( $\beta \gtrsim 0.274$ ; Durisen et al. 1986) after a stellar core formed. Otherwise, only a stellar core and stable disc form. However, in both papers, only the inner regions of the first hydrostatic core were modelled and the initial conditions were chosen somewhat arbitrarily. Ideally, to study the formation of close binary systems, one would wish to follow the collapse of an optically-thin, molecular cloud core all the way to stellar densities. However, such a calculation requires resolving densities from  $10^{-18} - 0.01$  g cm $^{-3}$  and length scales from  $\sim 10^{17} - 10^{10}$  cm in three dimensions.

To achieve such high spatial resolution in three dimensions we use the Lagrangian smoothed particle hydrodynamics (SPH) method. With SPH, the spatial resolution is given by the smoothing length (over which hydrodynamical properties are calculated) which in modern implementations is continuously variable (e.g. Benz et al. 1990). The smoothing lengths are set by ensuring that each particle contains a certain number of neighbours,  $N_{\text{neigh}}$ , or equivalently a fixed mass, within two smoothing lengths. Thus, in contrast to a grid-based code which has spatially-limited resolution, SPH has mass-limited

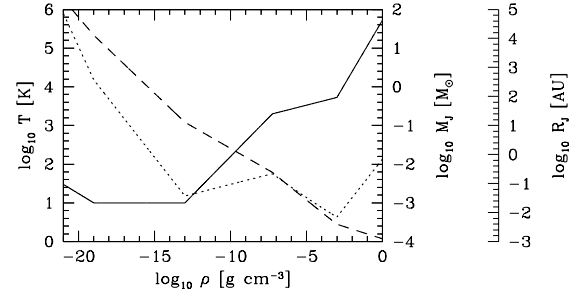


Fig. 1.— The gas temperature  $T$  (solid line), Jeans mass  $M_J$  (dotted line), and Jeans radius  $R_J$  (dashed line), as a function of density in a collapsing molecular cloud core (adapted from Tohline 1982). The minimum Jeans mass of  $\approx 4 \times 10^{-4} M_{\odot}$  occurs at the end of the second collapse phase when the dissociation of molecular hydrogen is almost completed at a density of  $\sim 10^{-3}$  g cm $^{-3}$ .

resolution which *automatically* gives greater spatial resolution in regions of higher density. Bate & Burkert (1997) recently demonstrated this mass-limited resolution. They found that to follow the collapse and fragmentation of a Jeans-unstable gas cloud reliably, the minimum resolvable mass should always be less than the Jeans mass (see also Whitworth 1998). In practice, this means that a Jeans mass should always be represented by at least  $\approx 2N_{\text{neigh}}$  particles.

The mass-limited resolution of SPH is ideal for studying the collapse and fragmentation of molecular cloud cores because there is a minimum Jeans mass in the problem (Figure 1). By contrast, there is no minimum Jeans length. This is a problem for grid-based codes which must resort to nested or adaptive grids (e.g. Burkert & Bodenheimer 1993; Truelove et al. 1998). With SPH, if the number of particles used is sufficient to resolve the minimum Jeans mass, a calculation can be followed to arbitrary densities with the required spatial resolution given automatically with increasing density.

## 2. Method

The calculations were performed using a three-dimensional SPH code based on a version originally developed by Benz (Benz 1990, Benz et al. 1990). The code uses a tree to calculate the gravitational forces and find nearest neighbours. The smoothing lengths are variable in time and space, subject to the constraint that the number of neighbours of each particle

must remain approximately constant at  $N_{\text{neigh}} = 50$ . The gravitational force between particles is softened over the hydrodynamic smoothing length using spline softening derived from the smoothing kernel. Hence, the gravitational softening length and hydrodynamic smoothing length are equal and decrease with increasing density. The standard form of the artificial viscosity is used (Monaghan & Gingold 1983), with the parameters  $\alpha_v = 0.5$  and  $\beta_v = 1.0$ . The SPH equations are integrated using a second-order Runge–Kutta–Fehlberg integrator. Individual time-steps are used for each particle (Bate, Bonnell & Price 1995). Further details can be found in the above references.

The code does not include radiative transfer. Instead, to model the behaviour of the gas during the different phases of collapse, we use a piece-wise polytropic equation of state  $P = K\rho^\gamma$ , where  $P$  is the pressure,  $\rho$  is the density,  $K$  gives the entropy of the gas, and the ratio of specific heats,  $\gamma$ , is varied as

$$\gamma = \begin{cases} 1 & \rho \leq 1.0 \times 10^{-13} \\ 7/5 & 1.0 \times 10^{-13} < \rho \leq 5.7 \times 10^{-8} \\ 1.15 & 5.7 \times 10^{-8} < \rho \leq 1.0 \times 10^{-3} \\ 5/3 & \rho > 1.0 \times 10^{-3} \end{cases} \quad (1)$$

where the densities are in  $\text{g cm}^{-3}$  (see Figure 1). The values of  $\gamma$  and the transition densities are derived from Tohline (1982). The variable value of  $\gamma$  mimics the following behaviour of the gas. The collapse is isothermal ( $\gamma = 1$ ) until the gas becomes optically thick to infrared radiation at  $\rho \approx 10^{-13} \text{ g cm}^{-3}$ , beyond which  $\gamma = 7/5$  (appropriate for a diatomic gas). When the gas reaches a temperature of  $\approx 2000 \text{ K}$  ( $\rho = 5.7 \times 10^{-8} \text{ g cm}^{-3}$ ), molecular hydrogen begins to dissociate and the temperature only slowly increases with density. In this phase we use  $\gamma = 1.15$  to model *both* the decreasing mean molecular weight and the slow increase of temperature with density, the latter of which has an effective  $\gamma \approx 1.10$ . Finally, when the gas has fully dissociated ( $\rho \approx 10^{-3} \text{ g cm}^{-3}$ ), the gas is monatomic and  $\gamma = 5/3$ . The value of  $K$  is defined such that when the gas is isothermal,  $K = c_s^2$  with  $c_s = 2.0 \times 10^4 \text{ cm s}^{-1}$ , and when  $\gamma$  changes the pressure is continuous.

To test that the above equation of state captures the important elements of the gas's behaviour, we have performed spherically-symmetric, one-dimensional (1-D), finite-difference calculations of the collapse of a molecular cloud core using the above equation of state and obtained excellent agreement with results from 1-D calculations incorporating radiative trans-

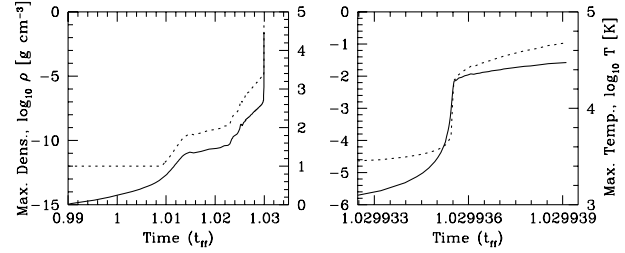


Fig. 2.— Maximum density (solid line) and maximum temperature (dotted line) versus time for the collapsing molecular cloud core. Time is given in units of the initial free-fall time ( $t_{\text{ff}} = 1.785 \times 10^{12} \text{ s}$ ). The right graph has expanded axes to show the second collapse phase in greater detail.

fer (e.g. Larson 1969; Winkler & Newman 1980a, b). We have also tested that the three-dimensional (3-D) SPH code can indeed accurately resolve the collapse down to stellar densities by performing comparison calculations with the same initial conditions as used by the 1-D finite-difference calculations. So long as the number of particles used by an SPH calculation is sufficient to resolve the Jeans mass throughout the calculation (see below), we obtain excellent agreement with the results from the 1-D finite-difference code. The details of these test calculations will be presented in a later paper.

### 3. Calculations

We present results from a 3-D SPH calculation following the collapse of an initially uniform-density, uniform-rotating, molecular cloud core of mass  $M = 1 \text{ M}_\odot$  and radius  $R = 7 \times 10^{16} \text{ cm}$ . The angular frequency is  $\Omega = 7.6 \times 10^{-14} \text{ rad s}^{-1}$ , and the ratios of the thermal and rotational energies to the magnitude of the gravitational potential energy are  $\alpha = 0.54$  and  $\beta = 0.005$ , respectively. To satisfy the resolution criterion of Bate & Burkert (1997), we require that the minimum Jeans mass during the calculation ( $\approx 4 \times 10^{-4} \text{ M}_\odot$ ) contains at least  $\approx 2N_{\text{neigh}} = 100$  particles. Hence, we use  $3 \times 10^5$  equal-mass particles.

The evolution of the calculation is as follows (Figure 2). The initial collapse is isothermal. When the density surpasses  $10^{-13} \text{ g cm}^{-3}$ , the gas in the center is assumed to become optically thick to infrared radiation and begins to heat ( $t = 1.009 t_{\text{ff}}$ ). The heating stops the collapse at the center and the first hydrostatic core is formed ( $t = 1.015 t_{\text{ff}}$ ) with maxi-

num density  $\approx 2 \times 10^{-11} \text{ g cm}^{-3}$ , mass  $\approx 0.01 M_{\odot}$  ( $\approx 3 \times 10^3$  particles), and radius  $\approx 7 \text{ AU}$ . As the first core accretes, its maximum density only slowly increases at first. However, the first core is rapidly rotating, oblate, and has  $\beta \approx 0.34 > 0.274$ , making it dynamically unstable to the growth of non-axisymmetric perturbations (e.g. Durisen et al. 1986). At  $t \approx 1.023 t_{\text{ff}}$ , after about 3 rotations, the first core becomes violently bar-unstable and forms trailing spiral arms. This leads to a rapid increase in maximum density as angular momentum is removed from the central regions of the first core (now a disc with spiral structure) by gravitational torques ( $t > 1.015 t_{\text{ff}}$ ). When the maximum temperature reaches 2000 K, molecular hydrogen begins to dissociate, resulting in a rapid second collapse to stellar densities ( $t = 1.030 t_{\text{ff}}$ ). The collapse is again halted at a density of  $\approx 0.007 \text{ g cm}^{-3}$  with the formation of the second hydrostatic, or stellar, core. The initial mass and radius of the stellar core are  $\approx 0.0015 M_{\odot}$  ( $\approx 5 \times 10^2$  particles) and  $\approx 0.8 R_{\odot}$ , respectively. Finally, an inner circumstellar disc begins to form around the stellar object, within the region undergoing second collapse. The calculation is stopped when the stellar object has a mass of  $\approx 0.004 M_{\odot}$  ( $\approx 1.2 \times 10^3$  particles), the inner circumstellar disc has extended out to  $\approx 0.1 \text{ AU}$ , and the outer disc (the remnant of the first hydrostatic core) contains  $\approx 0.08 M_{\odot}$  ( $\approx 2.4 \times 10^4$  particles) and extends out to  $\approx 60 \text{ AU}$ . Note that the massive outer disc forms *before* the stellar core. This final state is illustrated in Figures 3 and 4. If the calculation was evolved further, the inner circumstellar disc would continue to grow in radius as gas with higher angular momentum fell in. Eventually, the inner disc would meet the outer disc with only a small molecular dissociation region between the two.

The value of  $\beta$  during the second collapse, or after the stellar core and disc have formed, never exceeds the value necessary for dynamic instability to non-axisymmetric perturbations ( $\beta = 0.274$ ). Therefore, unlike in the calculations of Bonnell & Bate (1994), fragmentation to form a close binary system cannot occur. A similar result is obtained with  $\Omega = 3.4 \times 10^{-14} \text{ rad s}^{-1}$  and  $\beta = 0.001$  initially.

Since whether or not fragmentation can occur depends critically on the value of  $\beta$ , it is important that there has not been significant spurious transport of angular momentum by artificial viscosity or the diffusion of SPH particles. As SPH is a Lagrangian tech-

nique, it is relatively simple to keep track of the gravitational, pressure, and viscous torques on each particle. Thus, we can determine the cause of the change in angular momentum of a volume of gas between any two times. As one might expect, we find that there is virtually no angular momentum transport during dynamic collapse. Viscous evolution is more likely during the quasistatic evolution of the first core between its formation and the second collapse. In Figure 5, we consider the cause of the angular momentum transport during the quasistatic first core phase. Viscous evolution, which has presumably been active during the  $\approx 3$  rotations that the first core made before it became violently bar-unstable, is hardly detectable. By contrast, it takes only 1/4 of a rotation for gravitational torques to remove most of the angular momentum from the gas in the center of the core.

The absence of fragmentation could also be due to the value of  $\gamma$  during the second collapse being overestimated. This would lead to the value of beta that is achieved at the end of the collapse being underestimated. To determine the dependence of the results on  $\gamma$ , we performed calculations with  $\gamma$  as low as 1.05. This corresponds to an *isothermal* collapse but with the mean molecular weight still *decreasing* due to the dissociation of molecular hydrogen. In this extreme case  $\beta$  does briefly exceed 0.274 as the stellar core begins to form, but drops below the critical value again over approximately one rotation as the core increases in mass and before non-axisymmetric perturbations are able to grow significantly. The inner disc that forms around the stellar core also has a brief period with  $\beta > 0.274$  until more mass is accreted. Weak, transient spiral arms are visible in the disc over several rotations, however, there is no tendency for fragmentation.

#### 4. Conclusions

Larson (1969) performed the first hydrodynamical calculations of the collapse of a molecular cloud core to stellar densities using a spherically-symmetric, one-dimensional code. After nearly 30 years, it is now possible to perform three-dimensional calculations. Using SPH, we have followed the three-dimensional collapse of a molecular cloud core over 17 orders of magnitude in density contrast and 7 orders of magnitude in spatial extent, resolving both the isothermal and second collapse phases, and the formation of the first and second hydrostatic cores.

Using this technique, we have begun a study of whether or not close binary stellar systems may be formed during the second collapse phase of a molecular cloud core, as proposed by Bonnell & Bate (1994). We find that, if the first hydrostatic core is formed with sufficient rotational energy to make it dynamically unstable to the growth of non-axisymmetric perturbations, fragmentation during the second collapse is prevented because of the removal of angular momentum from the central regions of the first core via gravitational torques. The formation of close binaries during the second collapse phase *may be possible* for molecular cloud cores with different initial conditions, *especially* if they are rotating slowly enough that the first core is rotationally stable. Different initial conditions will be investigated in a subsequent paper.

## REFERENCES

Bate, M. R., Bonnell, I. A., & Price, N. M. 1995, MNRAS, 277, 362

Bate, M.R., & Burkert, A. 1997, MNRAS, 288, 1060

Benz, W. 1990, in The Numerical Modeling of Non-linear Stellar Pulsations: Problems and Prospects, ed. J. R. Buchler, (Dordrecht: Kluwer), 269

Benz, W., Bowers, R. L., Cameron, A. G. W., & Press, W. 1990, ApJ, 348, 647

Bonnell, I. A., & Bate, M. R. 1994, MNRAS, 271, 999

Boss, A. P. 1986, ApJS, 62, 519

Boss, A. P. 1988, ApJ, 331, 370

Boss, A. P. 1989, ApJ, 346, 336

Burkert, A., & Bodenheimer, P. 1993, MNRAS, 264, 798

Durisen, R. H., Gingold, R. A., Tohline, J. E., Boss, A. P., 1986, ApJ, 305, 281

Larson, R. B. 1969, MNRAS, 145, 271

Monaghan, J. J., & Gingold, R. A. 1983, J. Comput. Phys., 52, 374

Tohline, J. E. 1982, Fund. Cos. Phys., 8, 1

Truelove, J. K., Klein, R. I., McKee, C. F., Holliman, J. H., II, Howell, L. H., Greenough, J. A., & Woods, D. T. 1998, ApJ, 495, 821

Whitworth, A. P. 1998, MNRAS, 296, 442

Winkler, K.-H. A., Newman, M. J., 1980, ApJ, 236, 201

Winkler, K.-H. A., Newman, M. J., 1980, ApJ, 238, 311

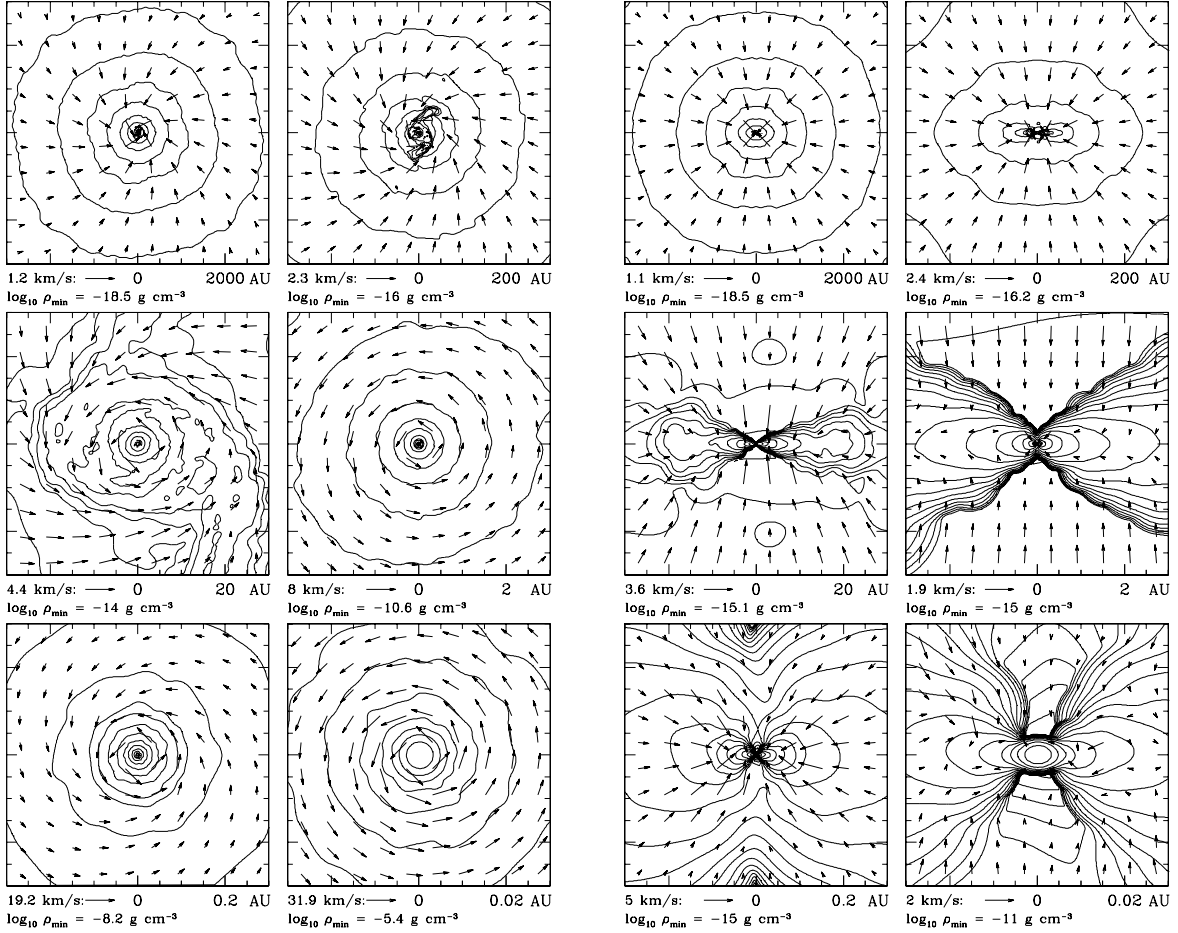


Fig. 3.— The state of the system at the end of the calculation. The six panels on the left give the density and velocity in the plane perpendicular to the rotation axis and through the stellar core. The six panels on the right give the density and velocity in a section down the rotation axis. In each case, the six consecutive panels give the structure on a spatial scale that is 10 times smaller than the previous panel to resolve structure from 3000 AU to  $\approx 0.2 R_\odot$ . The remnant of the first hydrostatic core (now a disc with spiral structure), the inner circumstellar disc, and the stellar core are all clearly visible. The distance scale (in AU), velocity scale (in  $\text{km s}^{-1}$ ), and logarithm of the minimum density (in  $\text{g cm}^{-3}$ ) are given under each panel. The maximum density is  $0.03 \text{ g cm}^{-3}$  and the logarithm of density is plotted with contours every 0.5 dex.

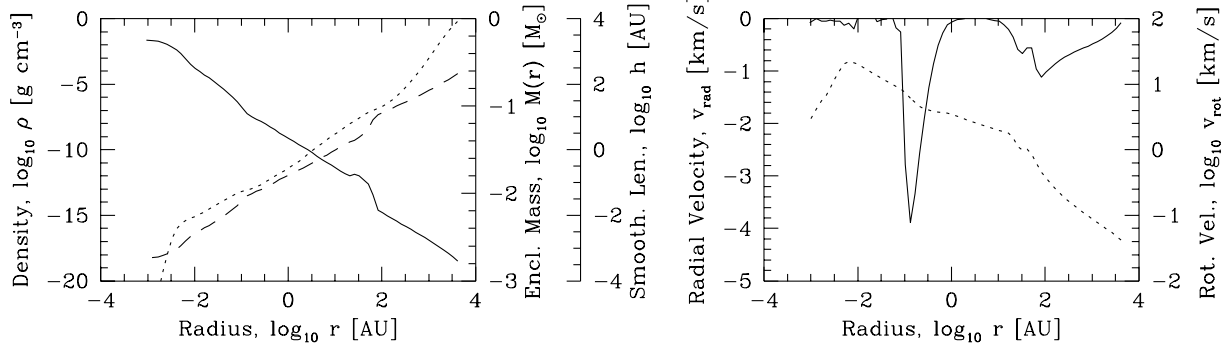


Fig. 4.— The state of the system at the end of the calculation. The left graph gives the density (solid line) and smoothing length (dashed line) as a function of radius and the mass enclosed within radius  $r$  of the center of the stellar core (dotted line). The right graph gives the radial (solid line) and rotational (dotted line) velocities as functions of radius from the center of the stellar core. The densities, smoothing lengths and velocities are the mean values in the plane perpendicular to the rotation axis and through the stellar core. The stellar core ( $r < 0.004$  AU), inner circumstellar disc ( $0.004 < r < 0.1$  AU), region undergoing the second collapse ( $0.1 < r < 1$  AU), outer circumstellar disc formed from the first core ( $1 < r < 60$  AU), and isothermal collapse region ( $r > 60$  AU) are clearly visible.

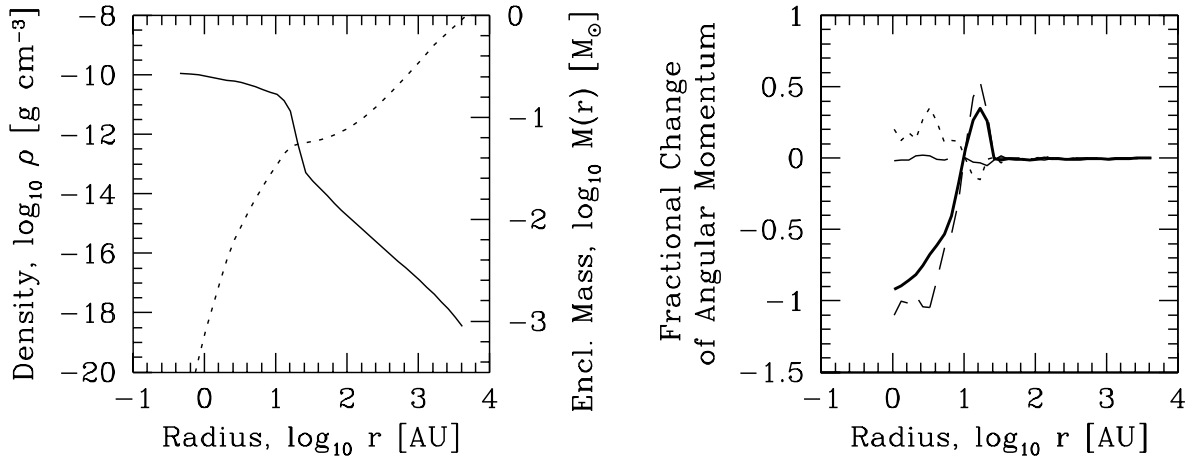


Fig. 5.— The cause of the change in angular momentum during the calculation. We show the system at  $t = 1.0234 t_{\text{ff}}$ . The first core has undergone approximately 3 rotations since its formation; it has been violently bar-unstable for just 1/4 of a rotation. The left graph gives the density as a function of radius (solid line) and the mass enclosed within radius  $r$  of the center of the first core (dotted line). The right graph shows the fractional change, since the beginning of the calculation, of the angular momentum of the gas as a function of radius (solid line), and the contributions to this change from gravitational (short-dashed line), pressure (dotted line) and viscous (long-dashed line) torques. Gravitational torques from the bar instability dominate the loss of angular momentum from the center of the first core; this angular momentum is deposited in the outer parts of the core. Pressure forces, due to the spiral arms, act to oppose the angular momentum transport. Viscous transport is negligible.